J Mater Sci (2007) 42:6331–6338
DOI 10.1007/s10853-006-1189-y

# Effects of modification and heat-treatment on the abrasive wear behavior of hypereutectic Al–Si alloys

**C. L. Xu · Y. F. Yang · H. Y. Wang · Q. C. Jiang**

Received: 20 May 2006 / Accepted: 30 October 2006 / Published online: 24 April 2007


**Abstract** In the present study, Al–Si alloys with Si contents of 23, 26, 28 and 31 wt.%, respectively, were modified with a new modifying agent. The results show that the primary silicon size decreased about 8–10 times after modification. The wear rates of the modified and heat-treated Al–Si alloys are lower than those of the unmodified and non-heat-treated Al–Si alloys, respectively. The silicon content in the range of 23–31 wt.% has a significant effect on the wear rates of the same processed Al–Si alloys (modification and heat treatment). Under the same load, the wear rates of the same processed Al–Si alloys decreased with the increasing silicon content. The abrasion took place mainly by cutting and partly by ploughing actions for the non-heat-treated Al–Si alloys, or on the contrary, mainly by ploughing and partly by cutting actions for heat-treated Al–Si alloys.

## Introduction

It is well known that the wear resistance of Al–Si casting alloys is higher than that of Al alloys due to the presence of hard silicon particles uniformly distributed throughout the matrix [1]. Recently, there is growing interest in hypereutectic Al–Si alloys because of their higher wear resistance and other interesting properties such as low thermal-expansion coefficient, good corrosion resistance and castability [2–5].

Considerable efforts have been devoted to studying the wear behaviors of the Al–Si alloys for a long time. Sarkar [6] carried out experiments on the Al–Si alloys (LM13 and LM29) under dry sliding against gray iron or steel and concluded that the hypereutectic Al–Si alloy wears more than the hypereutectic Al–Si alloy. Clarke and Sarkar [7] studied the wear characteristics of as-cast binary Al–Si alloys with Si contents varying up to 21 wt.%. They reported that the wear rates of near-eutectic Al–Si alloy were lower at various loads. However, Pramila Bai and Biswas [8] investigated the characterization of dry sliding wear of Al–Si alloys (4–24 wt.%Si) and found that the wear rates of the unmodified Al–Si alloys did not significantly differ under 0.105–1.733 MPa pressure and 0.19–0.94 m $s^{-1}$ speed. Recently, Torabian et al. [9] shown that the hardness of Al–Si alloys increases with the increase of the Si content, and under specific conditions of constant applied load and sliding velocity, the wear rate decrease as well. Prasad et al. [10] reported that the coarser primary silicon phase of gravity cast LM29 showed higher wear rates than the finer primary silicon phase of pressure cast LM29 due to a predominating embrittling effect and microcracking tendency brought about by the particles when tests were conducted against the fine abrasive.

Modification can change the morphology and size of primary silicon, eutectic silicon or both primary and eutectic silicon simultaneously. During heat treatment, eutectic silicon in hypereutectic Al–Si alloys disintegrated and spheroidized [11, 12]. According to Refs. [10, 13], the morphologies of silicon particles greatly influence the sliding wear behavior of the Al–Si alloys. But very limited information is available regarding the effects of modification and heat treatment on the abrasive wear behavior of

C. L. Xu · Y. F. Yang · H. Y. Wang · Q. C. Jiang (✉)
The Key Laboratory of Automobile Materials, Ministry of Education and Department of Materials Science and Engineering, Jilin University at Nanling Campus, No.142 Renmin Street, Changchun 130025, P. R. China
e-mail: jqc@jlu.edu.cn

the hypereutectic Al–Si alloys. Therefore, in the present study, an attempt was made to reveal the abrasive wear behaviors of differently processed Al–23 wt.%Si, Al–26 wt.%Si, Al–28 wt.%Si and Al–31 wt.%Si alloys.

## Experimental methods

The modifying agent used in the experiment consists of Al, P, Ti, TiC and Y (0.4P–10Ti–20TiC–0.8Y–Al balance, all in wt.%) [14]. The base alloys are Al–23 wt.%Si, Al–26 wt.%Si, Al–28 wt.%Si and Al–31 wt.%Si alloys, which were made by the addition of pure silicon (preheated at 400 °C for 2 h) into liquid Al–12 wt.%Si alloy. The chemical compositions of the Al–12 wt.%Si alloy and base alloys are given in Table 1. In the experiment, the base alloy was melted in a graphite crucible using an electric resistance furnace and then kept at temperature of 850 °C. Subsequently, the modifying agent was added into the melt and then the melt was stirred at 850 °C for approximately 5 min to ensure an adequate modification. The modified melt was poured into a metal mould preheated at 200 °C. Both unmodified and modified Al–Si alloys were solutionized in an air-forced furnace at 500 °C for 8 h, followed by quenching in hot water (~80 °C) and artificial ageing at 180 °C for 6 h.

In order to evaluate the effect of the differently processed Al–Si alloys on the sliding abrasive wear rates, dry sliding abrasive wear tests were performed using a pin-on-disc machine under loads ranging from 3 to 31 N at a sliding distance of 12.5 m. The differently processed Al–Si alloys with 6 mm in diameter and 12 mm in height were used as pin materials, and 1000 grit SiC abrasive papers (corresponding to 8 μm abrasive particles) were employed as the counterface. Before and after the test, the pin was cleaned with ethanol and weighed. The wear rate was calculated from the results of the weight loss, density and sliding distance. The metallographic samples, taken from the differently processed Al–Si alloys, were polished following the standard metallographic procedures and then were etched with 5% NaOH solution. Brinell hardness was measured using a 1,000 kg load and a 10 mm diameter indenter (HB $\leq$ 130), or a 750 kg load and a 5 mm diameter indenter (HB > 130), with a loading time of 30 s. A HIX-1000 type micro Vickers was used for Vicker hardness measurements. The load used was 25 g and loading time was 15 s. The presented value of Vicker hardness was taken from the average of five measurements. The density of the Al–Si alloys was measured using the Archimedean method.

The morphological features of the primary silicon and eutectic silicon in the Al–Si alloys were characterized using scanning electron microscopy (SEM), and the approximate compositions of the worn debris were identified by Energy-dispersive spectrometry (EDS).

## Results and discussion

### Microstructure and hardness

Primary silicon in the unmodified Al–Si alloys exhibits coarser platelet, star-like and other irregular morphologies as shown in Fig. 1(a). Figure 1(b) shows the effect of modifying agent on primary silicon in hypereutectic Al–Si alloys. When the modifying agent was added, the morphologies of the primary silicon were changed to a fine blocky shape. The sizes of the primary silicon in the modified hypereutectic Al–23 wt.%Si, Al–26 wt.%Si, Al–28 wt.%Si and Al–31 wt.%Si alloys are approximately average 20 μm, 20 μm, 28 μm and 35 μm, respectively, and in the unmodified Al–23 wt.%Si, Al–26 wt.%Si, Al–28 wt.%Si and Al–31 wt.%Si alloys are approximately average 200 μm, 200 μm, 250 μm and 250 μm, respectively. It is clear that the eutectic silicon in the unmodified and modified Al–Si alloys disintegrated and spheroidized during heat treatment as shown in Fig. 2(c) and (d). However, the morphologies of the primary silicon in the unmodified and modified Al–Si alloys were not changed by heat treatment as shown in Fig. 1(c) and (d). At the same time, it can be observed that the modifying agent did not have a significant effect on the eutectic silicon in the hypereutectic Al–Si alloys as shown in Fig. 2(b).

In order to reveal the effect of the Al–Si eutectic matrix on wear resistance, hardness (HV) measurements were performed, and the results are shown in Fig. 3. It is worth

**Table 1** Chemical compositions of Al–12 wt.%Si and base Al–Si alloys (wt.%)

| Material | Si | Fe | Cu | Mn | Mg | Zn | Ti | Others | Al |
|---|---|---|---|---|---|---|---|---|---|
| Al–12 wt.%Si alloy | 12.30 | 0.71 | 0.50 | 0.25 | 0.15 | <0.50 | <0.10 | <0.01 | Bal. |
| Al–23 wt.%Si alloy | 23.49 | 0.76 | 0.68 | 0.28 | 0.35 | 0.32 | <0.10 | <0.01 | Bal. |
| Al–26 wt.%Si alloy | 26.74 | 0.83 | 0.58 | 0.26 | 0.40 | 0.31 | <0.10 | <0.01 | Bal. |
| Al–28 wt.%Si alloy | 28.51 | 0.94 | 0.65 | 0.31 | 0.37 | 0.28 | <0.10 | <0.01 | Bal. |
| Al–31 wt.%Si alloy | 30.87 | 0.87 | 0.63 | 0.29 | 0.43 | 0.39 | <0.10 | <0.01 | Bal. |

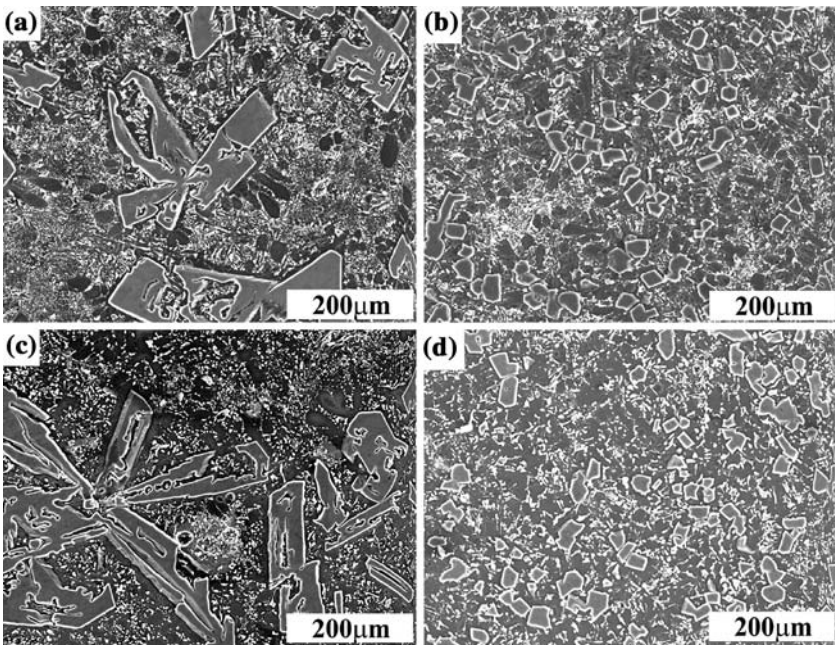


**Fig. 1** SEM micrographs of differently processed Al–28 wt.%Si alloys: (**a**) unmodified Al–28 wt%Si alloy, (**b**) modified Al–28 wt%Si alloy, (**c**) unmodified and heat-treated Al–28 wt%Si alloy and (**d**) modified and heat-treated Al–28 wt%Si alloy

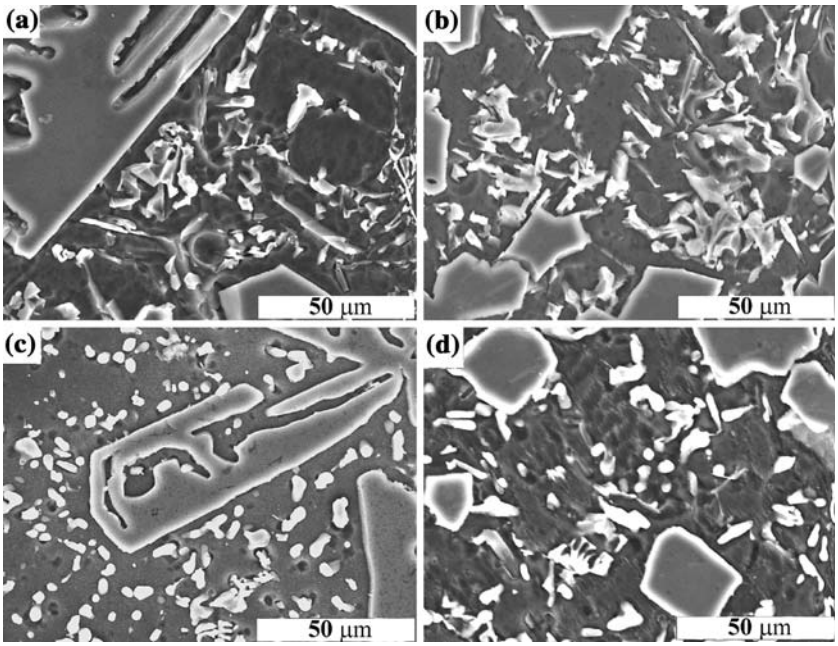


**Fig. 2** SEM micrographs of eutectic silicon in differently processed Al–28 wt.%Si alloys: (**a**) eutectic silicon in unmodified Al–28 wt%Si alloy, (**b**) eutectic silicon in modified Al–28 wt%Si alloy, (**c**) eutectic silicon in unmodified and heat-treated Al–28 wt%Si alloy and (**d**) eutectic silicon in modified and heat-treated Al–28 wt%Si alloy

noting that the Vickers hardness values of the Al–Si eutectic matrix of the non-heat-treated hypereutectic Al–Si alloys (both for unmodified and modified hypereutectic Al–Si alloys) are significantly lower than those of the heat-treated hypereutectic Al–Si alloys (both for unmodified and modified hypereutectic Al–Si alloys), and modification is helpful to improve Vickers hardness of the Al–Si eutectic matrix of the hypereutectic Al–Si alloys. The effects of the differently processed routes on the ambient temperature hardness (HB) of the hypereutectic Al–Si alloys are given in Fig. 4. The Brinell hardness values of the modified Al–Si alloys are higher than those of the unmodified Al-Si alloys, which are mainly due to the refinement of the primary silicon. On the other hand, the Brinell hardness values of the non-heat-treated hypereutectic Al–Si alloys are significantly lower than those of the heat-treated hypereutectic Al–Si alloys, which are partly attributed to the effect of heat treatment on the matrix.

## Wear rate

Figure 5 indicates that the wear rates of the investigated Al–Si alloys increase with the increasing load. Furthermore, it can be clearly observed that the wear rates of the

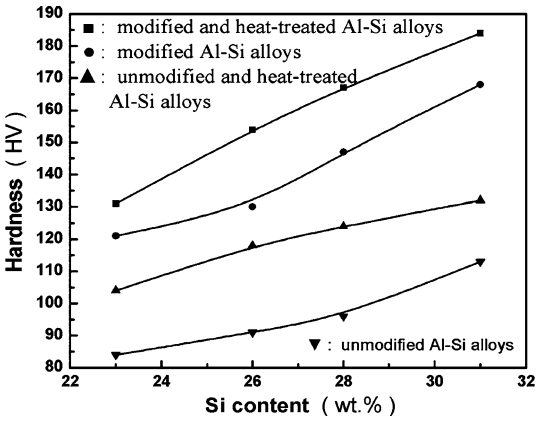


**Fig. 3** Hardness (HV) of Al–Si eutectic matrix of differently processed Al–Si alloys

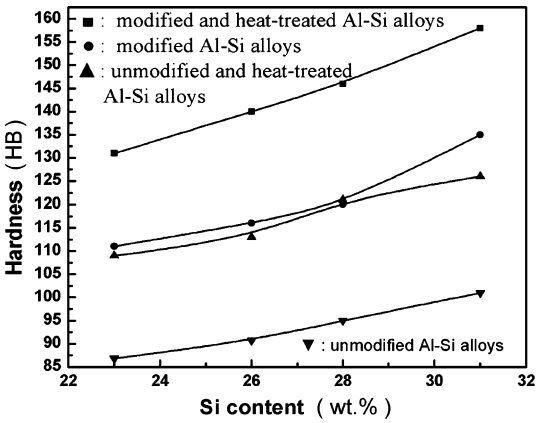


**Fig. 4** Hardness (HB) of differently processed Al–Si alloys

modified and heat-treated Al–Si alloys are lower than those of the unmodified and non-heat-treated Al–Si alloys under loads of 3–31 N, respectively. Therefore, it can be concluded that both the modification and the heat-treatment are beneficial to improve the wear resistance of the hypereutectic Al–Si alloys.

Previous studies have revealed that the wear behavior of the Al–Si alloys can be closely correlated to their microstructural features [10, 13, 15]. According to Ref. [16], the high wear resistance can be achieved by the presence of fine, well dispersed harder particles. So, the morphologies and the sizes of the primary and eutectic silicon in the hypereutectic Al–Si alloys play a critical role in determining the wear behavior of these alloys.

The heat-treatment leads to significant changes for the eutectic silicon in the microstructure. After the heat-treatment, the eutectic silicon (in both unmodified and modified Al–Si alloys) shows some spheroidizing effects, i.e., sharp corners have become rounded [11]. This effect can considerably relieve the localized stress concentration at spheroidized eutectic silicon/alpha aluminum interface. Therefore, during sliding abrasive wear, the spheroidized eutectic silicon phase in the heat-treated Al–Si alloys can effectively suppress crack propagation at the spheroidized eutectic silicon/alpha aluminum interface, making the spheroidized eutectic silicon be perfectly bonded by alpha aluminum and further enhancing the wear resistance of the heat-treated Al–Si alloys. Compared the non-heat-treated Al–Si alloys with the heat-treated Al–Si alloys, during sliding abrasive wear, the long needle-like eutectic silicon in the non-heat-treated Al–Si alloys aggravates the

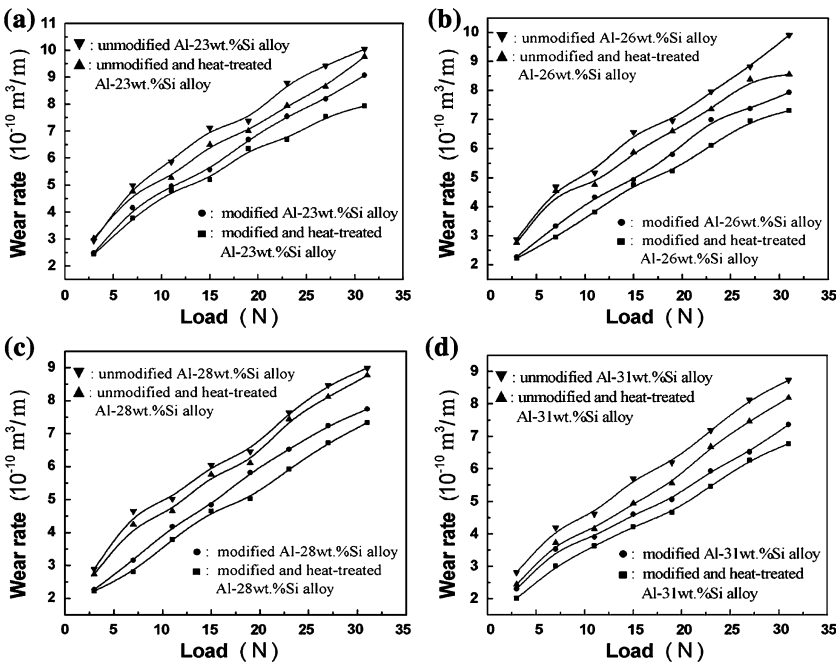


**Fig. 5** Wear rate as a function of applied load: (**a**) differently processed Al–23 wt.%Si alloys, (**b**) differently processed Al–26 wt.%Si alloys, (**c**) differently processed Al–28 wt.%Si alloys and (**d**) differently processed Al–31 wt.%Si alloys

localized stress concentration at the sharp corner of the eutectic silicon [17], which promotes cracks to initiate at the sharp corner of the needle-like eutectic silicon and propagate along the eutectic silicon/alpha aluminum interface. This result leads to the needle-like eutectic silicon to be poorly bonded by alpha aluminum and further reduce the wear resistance of the non-heat-treated Al–Si alloys. In addition, because the spheroidizing and coarsening of the eutectic silicon particles in the heat-treated Al–Si alloys can increase the fracture strain [18], the spheroidized and coarsened eutectic silicon particles become more difficult to fracture, which can effectively reduce the number of the crack nucleation sites. On the contrary, the needle-like eutectic silicon structure in the non-heat-treated Al–Si alloys is a ''network'' of plates which are more or less connected to each other. Therefore, the needle-like eutectic silicon structure leads to rapid reduction in the load-bearing area as some eutectic silicon phases crack and the cracks can propagate rapidly through the structure [19]. These may be one reason why the wear rates of the non-heat-treated Al–Si alloys are higher than those of the heat-treated Al–Si alloys.

In the experiments, the investigated Al–Si alloys contain numerous alloying and impurity elements, each of which has some effects on the structure and properties of the investigated Al–Si alloys. When the alloys are heat-treated and then followed by quenching, the solute components are retained in an unstable state. During the subsequent ageing and precipitation treatment at 180 °C for 6 h, the solute atoms are rejected and formed new phases as precipitate. The presence of the strained field around the new phases will limit the movement of dislocations, which can result in the increase in strength and hardness [20]. Both experimental results and theoretical considerations indicated [21] that the real number of contact $n$ (between abrasive paper and a metal counterface during two-body abrasive wear by fixed abrasive papers) was a function of the applied load $P$, the hardness of the wearing material $H$, the nominal contact area $A_0$ and the mean diameter of the abrasive particles $\bar{D}$. The relationship can be expressed as

$$n = k'\bar{D}^{-2}\left(\frac{P}{H}\right)^{1/2} A_0^{1/2}, \quad (1)$$

where $k'$ is a constant. According to this relationship, under the same $\bar{D}$, $P$ and $A_0$ condition, the hardness of the wearing material determines the real number of contacts $n$. From Eq. (1), it indicates that the real number of contacts $n$ will be less due to the higher hardness of the matrix. It is easy to understand that the average penetration depth of abrasive particles, an average result of all penetration depth of abrasive particles as shown in Fig. 6(a) and (b), decrease with the decrease in the real number of contacts $n$. During the two-body abrasive wear, the smaller average penetration depth leads to the quantities of material removed from the surface to be also decreased. Therefore, the wear rate decreases with the decrease in the real number of contacts $n$ due to the higher hardness of the matrix. This may be one reason why the wear rates of the heat-treated Al–Si alloys, under the same load, are lower than those of the non-heat-treated Al–Si alloys, which arises from the different hardness of the matrix as shown in Fig. 3. As mentioned above, modification is also useful to improve the ambient temperature hardness (HB) of the investigated hypereutectic Al–Si alloys. Namely, the fine and uniformly distributed primary silicon particles in the modified Al–Si alloys can have larger load-supporting ability than the coarse primary silicon in the unmodified Al–Si alloys. On the other hand, particle mean free path of primary silicon in the unmodified Al–Si alloy is larger than that in the modified Al–Si alloy as shown in Fig. 1(a) and (b). Generally, the larger particle mean free path of primary silicon can give rise to a deeper average penetration depth due to the lower load-supporting ability. Therefore, it can be deduced that the average penetration depth of abrasive particles will be deeper for the unmodified Al–Si alloys than the modified Al–Si alloys, which will aggravate the destructive action of the abrasive particles.

Evans and Wilshaw [22] reported that the brittle material removal by lateral fracture was assumed to occur when the lateral cracks, which were potential material removal sites, intersected from adjacent indenters. Therefore, lateral cracks were suggested to be an important mode of the brittle material removal during abrasive wear. Primary silicon phase in the hypereutectic Al–Si alloys belongs to brittle phase. It was also reported that the coarser primary silicon phase in the hypereutectic Al–Si alloys usually

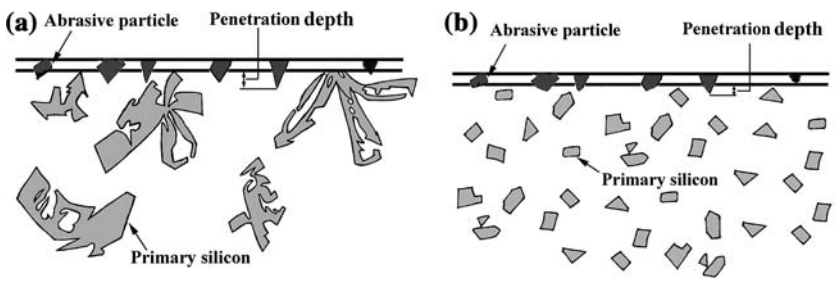


**Fig. 6** Schematic diagram shows destructive action of the abrasive particles to the worn surface: (**a**) unmodified alloys and (**b**) modified alloys

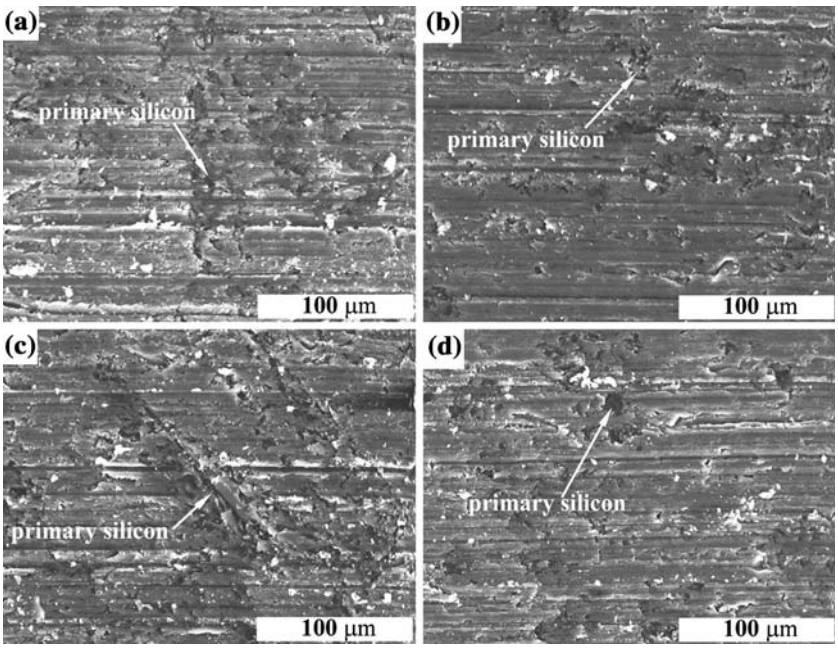


**Fig. 7** SEM micrographs of worn surfaces of differently processed Al–28 wt.%Si alloys under 15 N load: (**a**) unmodified Al–28 wt.%Si alloy, (**b**) modified Al–28 wt%Si alloy, (**c**) unmodified and heat-treated Al–28 wt%Si alloy and (**d**) modified and heat-treated Al–28 wt%Si alloy

leads to a higher wear rate than the finer primary silicon phase due to a predominating embrittling effect and microcracking tendency [10]. During two-body abrasive wear, therefore, the coarser primary silicon phase in the unmodified Al–Si alloys results in an increased probability of lateral fracture as shown in Fig. 7(a) and (c). In contrast, finer primary silicon phase in the modified Al–Si alloys can be effectively bound by the matrix, which decreased the microcracking tendency of the finer primary silicon phase, as shown in Fig. 7(b) and (d). These can conclude that the coarser primary silicon phase in the unmodified Al–Si alloys is easer to fracture and to be removed by the harder abrasive particles (SiC) from the matrix than the finer primary silicon in the modified Al–Si alloys. Subsequently, the fractured primary silicon particles in the unmodified Al–Si alloys, entrapped between the counterface and the alloys, may act as third-body abraders and aggravate the worn surface damage [23]. A strong bond between the finer primary silicon particles in the modified Al–Si alloys and the matrix [14] reduced the tendency for the finer primary silicon particles to be pulled out from the worn surface, which leads to less third-body wear during the wear process. On the other hand, a constancy of wear-surface profile is usually retained for a coarse two-phase material under steady-state conditions, as schematically illustrated in Fig. 8. The constancy indicates the wear behavior that the rate of material removal is the same for the two phases ($\alpha$ and $\beta$) regardless of their difference in abrasive behavior [24]. According to these analyses, the wear rate of the modified Al–Si alloy is lower than that of the unmodified Al–Si alloy, which is in accordance with the present study as shown in Fig. 5.

In the present study, the silicon content in the range of 23–31 wt.% has a significant effect on the wear rates of the same processed Al–Si alloys. Under the same load, e.g. 15 N, the wear rates of the same processed Al–Si alloys decreased with the increase in the silicon content as shown in Fig. 9. This can be attributed to the presence of the high volume fraction of the primary silicon phase, acting as a load-supporting element, in the same processed Al–Si alloys [23].

## Wear behavior

In order to reveal the wear behavior of the investigated Al–Si alloys, the worn surfaces of the samples and wear debris were examined under SEM. Figure 10 shows SEM micrograph of the wear debris generated at a load of 15 N. It can be clearly observed that the wear debris was mainly composed of submicron particles, and the morphologies of the wear debris of the differently processed Al–Si alloys

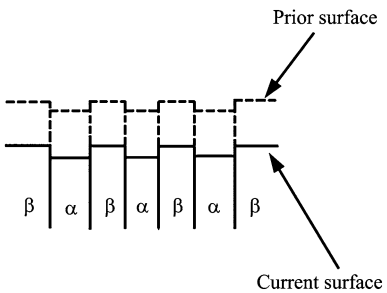


**Fig. 8** Schematic diagram shows that the two constituents of a composite material are worn at equal rates along the wear-surface normal direction [24]

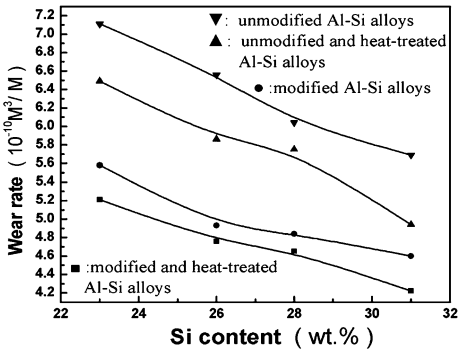


**Fig. 9** Wear rates of differently processed Al–Si alloys

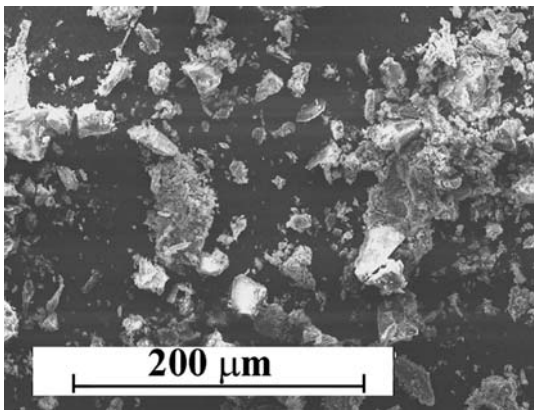


**Fig. 10** SEM micrograph of wear debris of Al–28 wt.%Si alloys under 15 N load

were similar. The EDS analysis demonstrated that the particles were mainly composed of aluminum, small amounts of silicon and aluminum oxides as shown in Fig. 11. Figure 7(a) to (d) shows the typical SEM micrographs of the worn surfaces of unmodified, modified, unmodified and heat-treated, modified and heat-treated

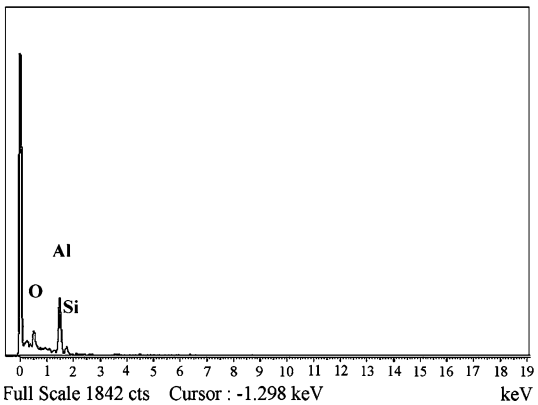


**Fig. 11** EDS analysis of the wear debris removed from the worn surface under 15 N load

Al–28 wt.%Si alloys under 15 N load, respectively. The worn surfaces are characterized by the presence of long grooves parallel to the motion direction of the abrasive papers and a few damaged regions. The abrasive particles slid over the surfaces of the investigated samples and formed grooves by cutting the surfaces of the investigated samples (in which material was directly removed from the worn surface) or pushing the matrix into ridges on the sides of the grooves (in which material was displaced on either side of the abrasion groove without removal). Sawla and Das [25] reported that the material of the hypoeutectic Al–Si alloys accumulated around the groove, deformed plastically, and was removed from the worn surface by nucleation and propagation of crack. In this experiment, during sliding abrasive wear, crack is easy to initiate at the sharp corner of the needle-like eutectic silicon (non-heat-treated) and propagates along the eutectic silicon/alpha aluminum interface, which can accelerate the nucleation and propagation of crack. Therefore, the Al–Si eutectic matrix (non-heat-treated) was removed from the worn surface mainly by cutting and partly by ploughing. However, the spheroidized eutectic silicon (heat-treated) was perfectly bonded by alpha aluminum, which can suppress the nucleation and propagation of crack. Therefore, the Al–Si eutectic matrix (heat-treated) was removed from the worn surface mainly by ploughing and partly by cutting. Because the abrasive particles (SiC) are harder than primary silicon, all of the primary silicon in the unmodified and modified Al–Si alloys will fracture and be removed from the worn surface during sliding abrasive wear. Therefore, the removed manners of the primary silicon in the unmodified and modified Al–Si alloys are almost the same.

## Conclusions

(1) The wear rates of the investigated Al–Si alloys increase with the increase in the loads. The wear rates of the modified and heat-treated Al–Si alloys are lower than those of the unmodified and non-heat-treated Al–Si alloys under the loads ranging from 3 to 31 N.

(2) The silicon content in the range of 23–31 wt.% has a significant effect on the wear rates of the same processed Al–Si alloys. Under the same load, e.g. 15 N, the wear rates of the same processed Al–Si alloys decrease with increase in the silicon content.

(3) The abrasion took place mainly by cutting and partly by ploughing action for the non-heat-treated Al–Si alloys, and mainly by ploughing and partly by cutting action for the heat-treated Al–Si alloys.

**Acknowledgements** This work was supported by the National Natural Science Foundation of China (No. 50531030) and the Ministry of Science and Technology of the People's Republic of China (No. 2005CCA00300) as well as the Project 985-Automotive Engineering of Jilin University.

## References

1. Lasa L, Rodriguez-Ibabe JM (2002) Scripta Mater 46:477
2. Gupta M, Ling S (1999) J Alloys Compd 287:284
3. Matsuura K, Kudoh M, Kinoshita H, Takahashi H (2003) Mater Chem Phys 81:393
4. Yang B, Wang F, Zhang JS (2003) Acta Mater 51:4977
5. Zhao HX, Cai J (1994) JOM 46(11):42
6. Sarkar AD (1975) Wear 31:331
7. Clarke J, Sarkar AD (1979) Wear 54:7
8. Pramila Bai BN, Biswas SK (1987) Wear 120:61
9. Torabian H, Patak JP, Tiwari SN (1995) J Mater Sci Lett 14:1631
10. Prasad BK, Venkateswarlu K, Modi OP, Yegneswaran AH (1996) J Mater Sci Lett 15:1773
11. Ogris E, Wahlen A, Lüchinger H, Uggowitzer PJ (2002) J Light Met 2:263
12. Lasa L, Rodriguez-Ibabe JM (2003) Mater Sci Eng A 363:193
13. Das S, Prasad SV, Ramachandran TR (1991) Mater Sci Eng A 138:123
14. Jiang QC, Xu CL, Lu M, Wang HY (2005) Mater Lett 54:624
15. Das S, Prasad SV, Ramachandran TR (1989) Wear 133:173
16. Zum Gahr KH (1979) Met Prog 116:46
17. Stolarz J, Foct J (2001) Mater Sci Eng A 319–321:501
18. Caceres CH, Griffiths JR (1996) Acta Mater 44:25
19. Pedersen L, Arnberg L (2001) Metall Mater Trans 32A:525
20. Haque MM, Sharif A (2001) J Mater Process Technol 118:69
21. Wang AG, Hutchings IM (1989) Wear 129:23
22. Evans AG, Wilshaw TR (1976) Acta Metall 24:939
23. Wang F, Liu HM, Ma YJ, Jin YS (2004) Mater Design 25:163
24. Liou JW, Chen LH, Lui TS (1995) J Mater Sci 30:258
25. Sawla S, Das S (2004) Wear 257:555